Talanta 291 (2025) 127766

Contents lists available at ScienceDirect

Talanta

journal homepage: www.elsevier.com/locate/talanta

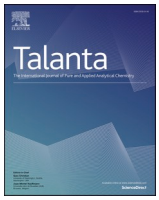

Enzymatic hydrolysis for pre-treating human serum before titanium dioxide nanoparticles assessment by spICP-MS

Ana Justo-Vega, Sara Vázquez-Pérez, Raquel Domínguez-González, Pilar Bermejo-Barrera, Antonio Moreda-Piñeiro *

Trace Elements, Spectroscopy and Speciation Group (GETEE), Institute of Materials (iMATUS), Department of Analytical Chemistry, Nutrition and Bromatology, Faculty of Chemistry. Universidade de Santiago de Compostela, Avenida das Ciencias, s/n, 15782, Santiago de Compostela, Spain

ARTICLE INFO

Keywords:
Titanium dioxide nanoparticles
Serum
Enzymatic hydrolysis
Ultra centrifugal filtration
spICP-MS

ABSTRACT

The current use of inorganic nanoparticles (NPs) in many industrial sectors, particularly in the food industry, has led to growing concerns about the toxicity of these emerging materials to humans. Therefore, NPs assessment in foodstuff, environmental materials and biological fluids is becoming an important topic, and the development of reliable quantification/characterization analytical methods is needed. The presence of NPs in blood and urine can be expected because of the bioavailability/assimilation of these entities by the organism. However, the determination of NPs in biofluids is a challenge mainly due to the complexity of the sample and the low levels of NPs (basal levels). The research on new methodologies for sample treatment is therefore needed.

The possibilities of enzymatic hydrolysis followed by centrifugal ultrafiltration for isolating titanium dioxide nanoparticles (TiO_2 NPs) from serum samples have been explored in the current research. Hydrolysis of serum's matrix components was performed with a pancreatin-lipase mixture (0.1 %(w/v) each one) operating at pH 7.4 and 37 °C for 4.0 h under orbital - horizontal shaking at 150 rpm. In addition, centrifugal ultrafiltration (30 kDa molecular weight cutoff (MWCO) membrane) was optimised for removing enzymes residues and other matrix's components. The developed method showed a limit of detection of 6.89×10^3 NPs mL^{-1}, and a limit of detection in size of 36 nm, whereas analytical recovery for spiking assays with 100 nm TiO_2 NPs were within the 103–114 % range.

1. Introduction

Titanium dioxide has long been used in paint formulations and coatings due to the bright white colour achieved in the final products. In addition, this pigment is also used as a white colorant in pharmaceuticals and foodstuff (referred as food additive E171 in the food industry), and in personal care products, mainly sunscreens, since the exhibited UV filter properties [1]. The food additive E171 has been demonstrated to contain up to 50 % titanium dioxide in nanometric state (titanium dioxide nanoparticles, TiO_2 NPs) [2], and the European Food Safety Authority (EFSA) has recently stated that E171 is not a safe food additive and hence, the use of E171 in the food industry is no longer authorized in the European Union [3]. The EFSA has also published a guidance for assessing the risk of the presence of nanomaterials (NMs) in the food/-feed chain [4], and several studies have demonstrated the high bio-persistence of TiO_2 NPs in human gastro-intestinal tract [5–7], and hence the potential distribution of TiO_2 NPs in several organs. In addition to ingestion (food chain), inhalation [8,9] and dermal and mucosal surface exposure [10] there are other exposure pathways for NMs, and several studies have been focused on occupational hygiene studies [8,9]. Therefore, the determination of NMs, mainly inorganic nanoparticles (NPs), in consumer products (foodstuff) and environmental materials is a challenging analytical problem which requires advances on analytical methodologies [11]. In addition, innovative analytical methods, including sample pretreatment, are required in nanotoxicological studies to determine the degree of NMs impregnation and bioavailability in humans.

Inductively coupled plasma-mass spectrometry (ICP-MS), mainly operating in the so-called single particle mode (spICP-MS) and single cell mode (scICP-MS), as well as other several ICP-MS-based systems, such as laser ablation-ICP-MS (LA-ICP-MS) and hyphenated ICP-MS techniques with hydrodynamic chromatography (HDC), capillary electrophoresis (CE) and flow field flow fractionation (FFFF) techniques, mainly asymmetrical FFFF (AF4), has been found to offer great potential

* Corresponding author.
E-mail address: antonio.moreda@usc.es (A. Moreda-Piñeiro).

https://doi.org/10.1016/j.talanta.2025.127766
Received 17 December 2024; Received in revised form 29 January 2025; Accepted 17 February 2025
Available online 28 February 2025

for determining and characterizing NPs in toxicological studies [12]. Several spICP-MS and ICP-MS-based methods for NPs assessment can be found in the literature [13–15], but applications focused on human biological fluids are scarce. The low concentration of NPs (basal levels) in biofluids, as well as he complexity of the sample, is a challenge in nanometrology, and robust and reliable sample pre-treatments and cleaning and/or preconcentration processes are needed. Developments have been mainly found for gold nanoparticles (Au NPs) in blood [16], blood serum and urine [17,18], and silver nanoparticles (Ag NPs) in blood [16,17,19], blood plasma [20], and urine [21]. Other developments have been performed for assessing platinum nanoparticles (Pt NPs) in human urine and blood serum [22], TiO_2 NPs in urine [21,23], and superparamagnetic iron oxide nanoparticles (SPIONs) [24] and carbon-coated iron carbide nanoparticles (C/Fe_3C NPs) [25] in simulated biological fluids.

Sample pre-treatment methods for isolating NPs from complex samples requires a soft environment for avoiding NPs degradation. Proposals for blood and blood serum have therefore consisted of using tetramethylammonium hydroxide (TMAH) at concentrations within the 1.0–5.0 %(v/v) range combined with 0.1 %(v/v) Triton X-100 [16,17,19,20,22] to digest the samples at room temperature [17,19] or at 4 °C [22] for 24 h. On other occasions, TMAH at 0.1 %(v/v) combined with 0.1 % (v/v) Triton X-100 and 2.8 %(v/v) NH_4OH 2.8 % (w/w) was also used for pre-treating blood under controlled temperature (37 °C) [20]. In addition, the analysis of blood and urine samples was conducted after dilution of the samples with a solution comprising ethylenediaminetetraacetic acid (EDTA), isopropyl alcohol, ammonia solution, and Triton-X100 [18]. Direct dilution with 1.0 %(v/v) glycerol for Ag NPs and TiO_2 NPs assessment [21] and 0.1 %(v/v) nitric acid for TiO_2 NPs [23] was also proposed for urine analysis.

Enzymes operate at mild temperatures and pH levels, promoting an extractive environment that ensures the integrity of the NPs. Combinations of pancreatin and lipase, as well as a multi-component enzyme mixture containing cellulose, hemicellulose and pectinase (Macerozyme R-10), have been proposed for isolating NPs from materials rich in proteins and fat such as seafood [26–29], and carbohydrates such as terrestrial plants and seaweed [30–32]. The aim of the current research has been the novel evaluation of enzymatic hydrolysis based on pancreatin and lipase mixtures for releasing TiO_2 NPs from serum structures. The extraction conditions of moderate pH and temperature minimise the degradation of TiO_2 NPs and the proposed sample pre-treatment may be useful for the extraction of other NPs that can be easily ionized. In addition, an additional step based on the centrifugal ultrafiltration (UF) has been originally used as a cleaning stage for removing degradation components from the enzymatic process. Characterization of TiO_2 NPs (particle size distribution) and quantification (particle number concentration) have been finally performed by spICP-MS.

2. Materials and methods

2.1. Instrumentation

Determinations were performed with a NexIon 2000 triple quadrupole ICP-MS system with dynamic reaction cell (DRC) technology from PerkinElmer (Waltham, MA, USA). The instrument is equipped with a Single Cell Micro DX autosampler (PerkinElmer), concentric Meinhard nebulizer attached to a cyclonic spray chamber (Glass Expansion, Inc., Melbourne, Australia), quartz torch with a quartz injector tube (2.5 mm i.d.), and triple cone system (nickel sampler cone, skimmer cone and hyperskimmer cone). Automatic data acquisition/management was performed with PerkinElmer Syngistix™ Nano Application 2.5 version software. Enzymatic hydrolysis was performed with a Rotabit orbital-rocking platform shaker (J.P. Selecta, Barcelona, Spain) placed inside a Boxcult temperature-controlled incubation chamber (Stuart Scientific, Surrey, UK). A Laborcentrifugen 2K15 centrifuge (Sigma, Osterode, Germany) equipped with a 12072 fixed-angle rotor was used for centrifugal filtration by using Amicon Ultra-4 centrifugal filter units (regenerated cellulose, 30000 NMWL) from Millipore (Cork, Irland). The same centrifuge equipped with a 12139-H fixed-angle rotor was used for solid removal when preparing enzymes solution. A F200-CF (Jeol, Tokyo, Japan) coupled to a Jeol JED-2300T were used for high resolution transmission electron microscopy (HRTEM) and energy dispersive X-rays spectrometry (EDX) analysis, respectively. A Kunft KMW-4459 domestic microwave oven (Shenzhen, China), with a microwave power of 700 W and programmable for time, was used for pre-treating the enzymatic extracts before TEM analysis. The poly(tetrafluorethylene) (PTFE) bombs were laboratory-made with hermetically sealed and resulted adequate to work at low pressures.

Other pieces of equipment were a Basic20 pH-meter (Crison, Barcelona, Spain), a Raypa UCI–150 ultrasonic cleaner water-bath (ultrasound frequencies of 17 and 35 kHz, power 325 W) from R. Espinar S.L. (Barcelona, Spain), a Reax orbital vortex stirrer (Heidolph, Schwabach, Germany), and a BP1215 analytical balance (Sartorius, Barcelona, Spain).

2.2. Reagents

All solutions/suspension were prepared with ultrapure water 18 MΩ cm of resistivity obtained from an IQ 7003 Milli-Q purification device (Millipore Co., Bedford, MA, USA). In addition, all glassware and plasticware were washed with ultrapure water, kept in 10 % (v/v) nitric acid for 48 h, and fully rinsed with ultrapure water before use for avoiding metal contamination.

Nanoparticle stock suspensions were prepared from 100 nm TiO_2 (nanopowder, rutile, 99.9 %) from US Research Nanomaterials (Houston, TX, USA). Gold nanoparticles suspensions used for assessing transport efficiency was prepared from a N8151035 standard (nanoComposix, San Diego, CA, USA) consisted of Au NPs covered by PEG carboxyl in aqueous 1.0 mM citrate with a certified particle diameter of 49.6 ± 2.1 nm, Au mass concentration of 12.4 ng mL^{-1}, and particle concentration of 9.89 × 10^6 Au NPs mL^{-1}. Ionic titanium [$(NH_4)_2TiF_6$ 1000 mg L^{-1}] and ionic gold ($AuCl_4$, 1000 mg Au L^{-1}) standard solutions were from Merck (Darmstadt, Germany) whereas, a NexION Setup Solution of Be, Ce, Fe, In, Li, Mg, Pb, and U at 10 μg L^{-1} (used for instrument tunning) was from PerkinElmer (Waltham, MA, USA). The enzymatic solution was prepared from porcine pancreatin and lipase from *Candida rugose* (Sigma Aldrich, Osterode, Germany) and using a 0.2 M sodium dihydrogen phosphate (NaH_2PO_4) solution prepared from NaH_2PO_4 (Merck) and adjusting the pH to 7.4 using a 0.2 M sodium hydroxide (NaOH) solution prepared from NaOH (Merck). Diluted glycerol solutions (1 %(v/v)) were prepared from 99.5 % glycerol from Sigma Aldrich.

2.3. Human serum samples

Serum samples (30 samples of approximately 2.0 mL each from different patients) were supplied by the Central Laboratory at the Santiago de Compostela University Hospital Complex (CHUS) in compliance with the ethical criteria stablished by the centre regarding patient anonymity. Several pooled serum samples were prepared by combining four-five serum samples before freezing at −20 °C. Each pooled serum sample ensures matrix homogeneity and the same basal TiO_2 NPs content for further optimization experiments.

2.4. Enzymes mixture preparation

A solution containing 0.1 %(w/v) pancreatin and 0.1 %(w/v) lipase was prepared by dissolving/suspending the appropriate amounts of enzymes in a 0.2 M NaH_2PO_4 solution (pH adjusted at 7.4 with a 0.2 M NaOH solution). The mixture was further sonicated (35 kHz, 325 W) for 5.0 min to ensure enzymes dissolution. Pancreatin was found to be

slightly soluble, and undissolved enzyme was removed by centrifugation (3900 rpm, 10 min) for preventing TiO_2 NPs agglomeration as consequence of pancreatin slurries and avoiding obstruction of the ultrafiltration membrane. The dissolved portion of the enzyme's mixture was used for further experiments.

2.5. Enzymatic hydrolysis process

Serum samples (0.5 mL) were mixed with 4.0 mL of an enzyme's solution at 0.1 %(w/v) pancreatin and lipase each one (prepared in 0.2 M NaH_2PO_4, pH at 7.4 with 0.2 M NaOH) and subjected to orbital – horizontal shaking at 150 rpm and at 37 °C for 4.0 h. Three replicates were performed for each set of conditions together with a reagent blank.

2.6. Centrifugal ultrafiltration process

The hydrolysed serum is charged into ultrafiltration tubes (30 kDa NMWL) and centrifugation at 3900 rpm (2364 g) and 20 °C is performed for 40 min. This stage ensures TiO_2 NPs retention whereas, hydrolysed serum components are removed by passing through the membrane. The concentrate in the filter container was recovered by placing the filter container upside down in a clean microcentrifuge tube and centrifuging at 3900 rpm (2364 g) and 20 °C for 2 min. The recovered hydrolysed serum (around 50–100 μL) was further diluted to 2.0 mL and 1.0 mL with a glycerol solution at 1 %(v/v) for optimization and validation assays, respectively.

The experimental workflow for the overall method (enzymatic hydrolysis and UF) is given in Fig. 1.

2.7. Operating conditions for spICP-MS determination of TiO_2 NPs

Daily performance of the ICP-MS instrument was assessed by monitoring Be, In, U, Ce (Ce^{++}/Ce and CeO/Ce ratios) and background in accordance with ICP-MS manufacturer. Determinations were performed using ammonia (flow rate of 1.0 mL min^{-1}) as a reaction gas (Table 1) to monitor an ammonia cluster at *m/z* 131 ($^{48}Ti(NH)(NH_3)_4$) [33]. Therefore, the quadrupole ion deflector (axial field voltage, AFT at 350 V), RPa (high-mass cut-off) and RPq (low-mass cut-off) rejection parameters were fixed at optimised values (Table 1) for a better focusing of the mass-to-charge ratio of the ammonia adduct.

The particle frequency method [34] was used for assessing the transport efficiency (TE%). Therefore, the sample flow rate (obtained values within the 0.19–0.21 mL min^{-1} range) was calculated by aspirating ultrapure water and weighing the solution before and after aspiration at the selected pump conditions). In addition, an aqueous ionic Au calibration (within the 0.5–10 μg L^{-1} range), and the measurement of an Au NPs suspension (9.89 × 10^4 particles mL^{-1}) were performed. Transport efficiency (TE%) values, directly calculated by PerkinElmer Syngistix™ Nano Application 2.5, were between 7.8 and 10.3 %.

Table 1
Operating conditions for spICP-MS analysis.

Analyte (*m/z*)	Ti (131)
Density (g cm^{-3})	4.23
Mass Fraction	59.90 %
Sample Flow Rate (mL min^{-1})	0.18–0.21
Transport efficiency (%)	8.0–10.0
Dwell time (μs)	100
Mode	Dynamic Reaction Cell Technology
Ammonia flow rate (mL min^{-1})	0.75
Ion-product registered	$^{48}Ti(NH)(NH_3)_4$
Rejection parameter q	0.20
Quadrupole ion deflector (V)	Set for maximum ion transmission

Calibrations were performed using ultrapure water and covering dissolved (ionic) titanium concentrations of 2.5, 5.0, 10.0, 15.0, and 20.0 μgL^{-1}. The enzymatic digests were conveniently diluted with 1.0 % (v/v) glycerol (dilutions varied from 5 to 10), and solutions were subjected to ultrasounds (ultrasound water-bath, 37 kHz) for 2.0–3.0 min before spICP-MS measurements (operating conditions summarized in Table 1). TiO_2 NPs particle number concentration and size distribution were directly obtained from PerkinElmer Syngistix™ Nano Application 2.5 considering the TiO_2 mass fraction of 59.90 % and TiO_2 density of 4.23 g cm^{-3} (Table 1) and by assuming a spherical nature of the TiO_2 NPs.

2.8. High resolution transmission electronic microscopy and EDX analysis

The high organic matter content in the enzymatic extracts from serum samples impair the HRTEM-EDX analysis of extracts, and a procedure for removing organic matter is needed before analysis. Therefore, the enzymatic extracts from spiked serum samples were subjected to an oxidative procedure involving 33 %(v/v) hydrogen peroxide and microwave heating in accordance with Taboada-López et al. [27]. Then, the cleaned enzymatic digests (10 μL) were dropped onto a copper grid, wicked on filter paper, and air-dried at room temperature before HRTEM-EDX analysis.

Regarding 100 nm TiO_2 NPs standard, a suspension at 250 mg L^{-1} (TiO_2 NPs mass concentration) of the material was dispersed under ultrasound, and 10 μL were dropped onto a copper grid (also wicked on filter paper and air-dried at room temperature) before direct HRTEM-EDX measurement.

3. Results and discussion

3.1. Optimization of the enzymatic hydrolysis process

In addition to various substances such as nutrients, hormones and metabolic waste, the main components of serum are ions acting as

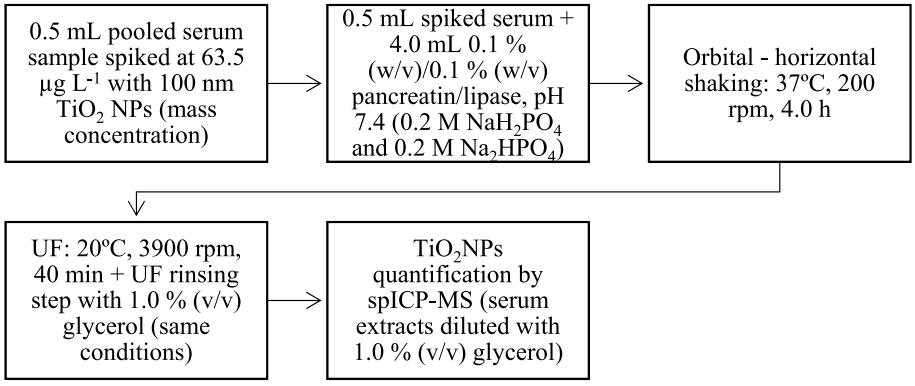

Fig. 1. Schematic diagram of the experimental workflow followed.

electrolytes, proteins (including antibodies) and lipids (cholesterol) [35]. Therefore, a proteolytic enzyme (pancreatin) and lipase were selected to hydrolyse the serum matrix and release TiO_2 NPs. Inherent variables affecting pancreatin and lipase activity, such as temperature and pH, were fixed at the optimum (recommended) values of 37 °C and 7.4 for maximum hydrolysis efficiency. Ionic strength, another important parameter in enzymatic hydrolysis procedures, was settled by the concentration of the buffer's components used for fixing the pH (0.2 M NaH_2PO_4 and 0.2 M Na_2HPO_4). The effect of other variables that can influence the hydrolysis process, such as enzyme (pancreatin plus lipase) concentration, hydrolysis time, and shaking rate, have been conveniently studied. Since the direct serum analysis gave TiO_2 NPs number concentrations lower than the limit of detection (LOD) of the method, spiked serum samples were used for optimization proposals. Spiking experiments have consisted of adding a convenient volume of a 100 nm TiO_2 NPs suspension to pooled serum sample to achieve a spiked concentration of 63.5 μg L^{-1}. Then, 0.5 mL of the spiked serum samples were mixed with 4.0 mL of the enzymes solution (variable concentrations depending on the tested condition). Experiments were performed in triplicate.

Recovered TiO_2 NPs contents used for discussing the optimization and validation assays (also TiO_2 NPs contents displayed in plots) throughout this research were based on TiO_2 mass concentration instead of TiO_2 particle number concentration. A spherical shape of TiO_2 NPs using the mean diameter of the particle size distribution (given by spICP-MS), and the TiO_2 particle number concentration (also given by spICP-MS) was assumed for obtaining TiO_2 mass concentrations (expressed as μg L^{-1}). The effect of TiO_2 agglomeration (changes on the mean sizes) is therefore minimised by considering TiO_2 mass concentrations rather than TiO_2 number concentrations. Finally, the cleaned extracts after UF were diluted to 2.0 mL with 1.0 %(v/v) glycerol.

An additional remark is referred to the size distribution of the 100 nm TiO_2 NPs standard used in the current research. As it can be seen in the HRTEM image (Fig. 2(a)), the material shows a high degree of agglomeration, and the right particle size assessment is quite difficult. Data obtained by applying the spICP-MS methodology (see next sections) will reveal most frequent sizes around 150 nm and mean sizes 160–180 nm. The EDX analysis (Fig. 2(b)) shows the characteristic peaks at 4.50 keV (TiK_a) and 5.0 keV (TiK_b) which implies the presence of Ti.

3.1.1. *Effect of the pancreatin/lipase concentration*

A first set of experiments were conducted to select the amounts of enzymes (pancreatin and lipase) by preparing buffered solutions at pH 7.4 containing 0.100, 0.250, 0.375, and 0.500 %(w/v) of each enzyme. The mixtures (0.5 mL of serum and 4.0 mL of enzymes solution) were subjected to an orbital-horizontal shaking at 150 rpm and at 37 °C for 14 h. After hydrolysis, the enzymatic digests were subjected to a UF step followed by with two UF rinsings stages with 1.0 %(v/v) glycerol. The retentate solution was recovered and diluted to 2.0 mL with 1.0 %(v/v) glycerol. Results (mean TiO_2 NPs mass concentration and mean size) of three replicates after blank subtraction are plotted in Fig. 3(a) and a gradual decreased on the TiO_2 mass concentration was obtained when increasing the enzymes concentration. In parallel, hydrolysis using high enzyme concentrations leads to a gradual increased on the measured sizes (Fig. 3(a)). These findings can be explained considering the agglomeration phenomena. Aggregation of TiO_2 NPs has been reported to be affected by pH, ionic strength, and dissolved (inorganic and organic) compounds [36–38]. Elevated enzyme concentrations have been demonstrated to result in increased enzyme residue concentrations, a factor that has been hypothesised to promote the agglomeration of TiO_2 NPs. In addition, the best results when using low extractant (enzyme) concentrations agree with previous papers regarding the use of low TMAH concentrations for TiO_2 NPs extraction from seafood [39] and also for Pt NPs, Au NPs and Ag NPs from biofluids [16,17,19,20,22], as well as low enzyme concentrations for isolating TiO_2 NPs and Ag NPs from seafood [26–29,31,32]. Therefore, pancreatin and lipase concentration was fixed at 1.0 %(w/v), experiments which led to a TiO_2 NPs mass concentration of 23.8 ± 1.7 TiO_2 μg L^{-1} (value quite lower than the TiO_2 NPs mass concentration used for spiking experiments, 63.5 TiO_2 μg L^{-1}).

3.1.2. *Effect of the hydrolysis time and the orbital-horizontal shaking rate*

After fixing the concentration of pancreatin and lipase at 0.1 %(w/v), spiked serum samples were subjected to enzymatic hydrolysis (orbital-horizontal shaking at 150 rpm) for several times (from 1.0 to 14 h). Also, the enzymatic digest was subjected to UF and two UF rinsing stages (use of 1.0 %(v/v) glycerol). Fig. 3(b) shows that recovered TiO_2 NPs remains constant for hydrolysis times higher than 4.0 h (TiO_2 NPs mass concentrations of 26.0 ± 1.3, 24.0 ± 2.4, and 25.3 ± 2.2 TiO_2 μg L^{-1} for 4.0, 6.0, and 14.0 h, respectively). Therefore, a hydrolysis time of 4.0 h was selected.

By fixing the hydrolysis time at 4.0 h and the enzymes amount (0.1 %(w/v)), the effect of the orbital-horizontal shaking rate was evaluated. An UF stage followed by two UF rinsings with 1.0 %(v/v) glycerol was performed in triplicate for spiked serum samples, and results after spICP-MS analysis are plotted in Fig. 3(c). The orbital-horizontal shaking rate was found to slightly increase the recovered TiO_2 NPs mass concentration up to 32.1 ± 1.9 TiO_2 μg L^{-1} when using the highest orbital-

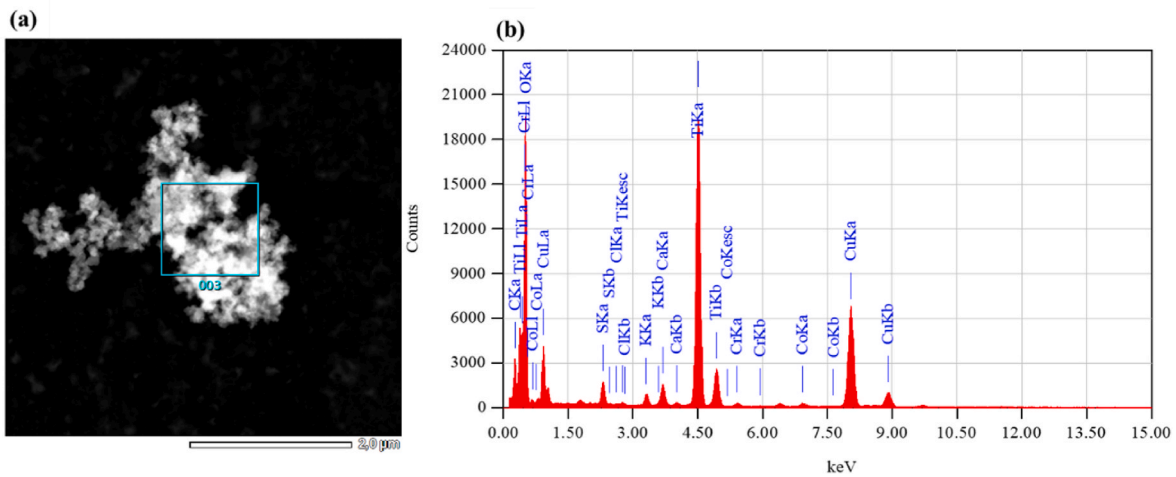

Fig. 2. HRTEM image (a) and EDX spectrum showing Ti characteristic peaks at 4.5 keV (TiK_a) and 5.0 keV (TiK_b) (b) of a slurry containing 100 nm TiO_2 NPs standard at 10 mg L^{-1} TiO_2 NPs.

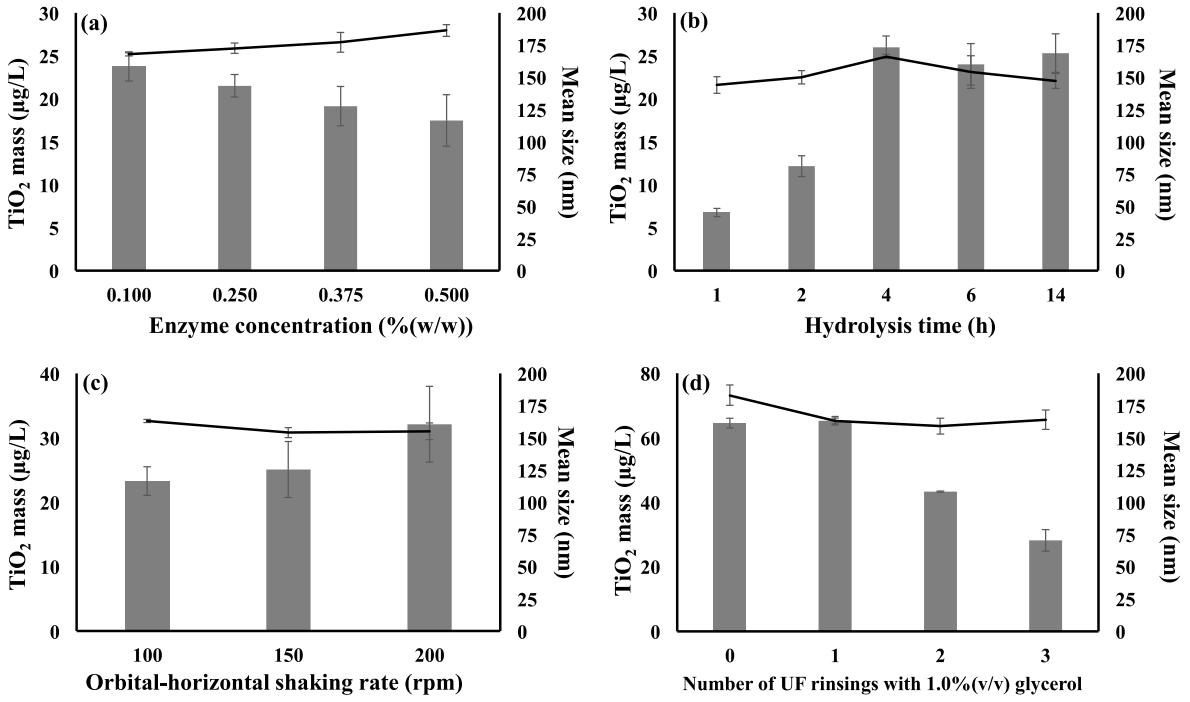

Fig. 3. Effect of the enzyme (pancreatin plus lipase) concentration (a), hydrolysis time (b), orbital-horizontal shaking rate (c), and number of UF rinsings (d) on the TiO_2 NPs mass concentration (bars referred to the left *Y* axis) and mean size (lines referred to the right *Y* axis) for serum samples spiked with 63.5 µg L^{-1} TiO_2 NPs (n = 9).

horizontal shaking rate tested (200 rpm). Furthermore, similar TiO_2 NPs size distributions were observed in the 154–163 nm range as shown in Fig. 3(c). The slightly better increase on recovery could be attributed to better mixing at high shaking rates.

3.1.3. *Effect of the number of UCF rinsings*

After fixing the parameters involved in the enzymatic hydrolysis process, the effect of the number of 1.0 %(v/v) glycerol UF rinsings was evaluated. Fig. 3(d) shows that two successive rinses UF promotes TiO_2 NPs losses, and the highest TiO_2 NPs mass concentrations were achieved when omitting the 1.0 %(v/v) glycerol rinsing or at least when using only one glycerol UF rinsing (TiO_2 NPs mass concentrations of 65.3 ± 1.3 TiO_2 µg L^{-1} for one UF rinsing and 64.5 ± 1.5 TiO_2 µg L^{-1} without UF rinsing). These findings suggest that TiO_2 NPs losses can occur during the UF cleaning stage, and further investigations would be necessary to establish whether TiO_2 NPs loss is due to retention by adsorption on the cut-off membrane and/or TiO_2 NPs passage of NPs through the cut-off membrane.

Regarding TiO_2 NPs size distribution, higher mean sizes (183 ± 8 nm) were achieved in absence of UF rinsings, whereas the mean values decrease within the 159–164 nm when performing the glycerol rinsings. Therefore, one UF rinsing with 1.0 %(v/v) glycerol was finally selected to clean the enzymatic extract and to diminish TiO_2 NPs agglomeration since the presence of biomolecules residues.

3.2. *Analytical performances*

A preliminary study for TE% assessment was performed by preparing Au NPs slurries (9.89×10^4 parts mL^{-1}) in ultrapure water and in 0.1 % (w/v) pancreatin and 0.1 %(w/v) lipase. Values for TE% were found to be quite similar (9.18 ± 0.95 %, within the 7.77–10.30 % range, n = 9, for Au NPs slurries in ultrapure water, and 8.57 ± 0.77 %, within the 7.58–9.40 % range, n = 4, for Au NPs slurries in 0.1 %(w/v) pancreatin and 0.1 %(w/v) lipase).

Similarly, a comparison between calibration slopes and recovered TiO_2 NPs when using ionic Ti calibrations in ultrapure water and in 0.1 %(w/v) pancreatin and 0.1 %(w/v) lipase was also tested. Ionic Ti concentration ranged from 2.5 to 20.0 µg L^{-1} (TiO_2 NPs mass concentration) for all cases, and good linearity ($R^2 > 0.9947$) was observed. Calibration slopes of nine aqueous calibration curves and four matched enzymes (pancreatin plus lipase 0.1 %(w/v) each one) were 0.413 ± 0.0506, and 0.330 ± 0.082, respectively, which implies that aqueous Ti standards can be used for measurements. This fact has been verified after analysing by sextuplicate TiO_2 NPs slurries at 127.0 µg L^{-1} (TiO_2 NPs mass concentration) by using both calibration methods since measured/recovered TiO_2 NPs were 126.7 ± 3.5 µg L^{-1} for aqueous standards and 129.4 ± 3.4 µg L^{-1} for matched calibrations. Similarly to TE%, enzymatic digest composition, even at high enzyme concentrations as 0.1 % (w/v), and matrix effect can be considered negligible after diluting the enzymatic digests with 1.0 %(w/w) glycerol.

The limit of detection for particle size (LOD_{size}) and particle number concentration (LOD_{NP}) was stablished in accordance with Laborda et al. [40] by considering the 5σ (5 × baseline standard deviation) criterion, which guarantees the avoidance of false positives (NP distributions partially overlapped with the background) [41]. Values of 36 nm and 5.70×10^3 particles mL^{-1} were obtained for LOD_{size} and LOD_{NP}, respectively. The LOD_{size} after applying this criterion was quite close to the LOD_{size} daily given by Syngistix™ Nano Application 2.5 version software (LOD_{size} within the 34–41 nm range).

The precision was studied with spiked serum samples at two different 100 nm TiO_2 NPs mass concentrations (63.5 and 127.0 µg L^{-1}) which were subjected to the enzymatic hydrolysis and UF process in triplicate followed by spICP-MS analysis also in triplicate. Precision, expressed as the relative standard deviation (%RSD) for nine measurements, was 14 and 7 % for spiked samples at 63.5 and 127.0 µg L^{-1}, respectively.

Accuracy of the method was assessed through analytical recovery by spiking serum samples with 100 nm TiO_2 NPs at 63.5 and 127.0 µg L^{-1} (spiking experiments in triplicate) and subjecting the spiked serum samples to the enzymatic hydrolysis and UF procedures. Replicated measurements (n = 3) of the un-spiked and spiked serum samples were used for calculating the analytical recovery in accordance with equation (1)

$$\%\,AR = \frac{[TiO_2\ NP]_{spiked} - [TiO_2\ NP]_{unspiked}}{[TiO_2\ NP]_{standard}} \times 100 \quad (1)$$

where $[TiO_2\ NP]_{spiked}$ is the TiO_2 NPs concentration in the spiked serum (part mL^{-1}), $[TiO_2\ NP]_{unspiked}$ is the TiO_2 NPs concentration in the serum blank (part mL^{-1}), and $[TiO_2\ NP]_{standard}$ is the TiO_2 NPs concentration of the standard suspension used for spiking experiments.

It should be noted that un-spiked serum samples gave TiO_2 NPs mass concentrations lower than the LOD_{NP} of the method. Values, expressed as mean ± standard deviation, were 105 ± 11 % and 113 ± 8 % for spiked serum samples at 63.5 and 127.0 μg L^{-1}, respectively.

3.3. Applications

Four different serum samples were subjected to the optimised procedure in triplicate, but TiO_2 NPs number concentrations were found to be lower than the LOD_{NP} of the method (5.70×10^3 particles mL^{-1}) for all cases. A further application was then performed by spiking in triplicate a serum sample with 100 nm TiO_2 NPs (63.5 μg L^{-1}, TiO_2 NPs mass concentration). Determinations by spICP-MS in triplicate were performed after enzymatic hydrolysis for 4.0 h and UF and without enzymatic hydrolysis (enzymes mixture was added but the serum samples were immediately subjected to UF – referred as time 0 h in Table 2). Determinations of TiO_2 NPs were found to be improved after applying the enzymatic hydrolysis procedure (51.6 ± 5.2 μg L^{-1} without enzymatic hydrolysis and 61.1 ± 2.1 μg L^{-1} with enzymatic hydrolysis) which led to enhanced analytical recoveries (82 ± 8 % without enzymatic hydrolysis and 97 ± 3 % with enzymatic hydrolysis).

Regarding size distributions, Table 2 shows that TiO_2 NPs sizes remained unchanged since the calculated most frequency size was 146 ± 15 and 146 ± 7 nm in absence and presence of enzymatic hydrolysis, respectively (Table 2). However, a little difference has been observed in the mean sizes which varied from 169 ± 15 nm in absence of enzymatic hydrolysis to 180 ± 7 nm when applying the enzymatic process. Since the most frequent sizes are smaller than the mean sizes, a positively skewed size distribution was observed (Fig. 4) and the most frequency size is preferable because it is unaffected by extreme outliers. Additionally, HRTEM images and EDX analysis for TiO_2 NPs in spiked serum samples without enzymatic hydrolysis and with UF, and after enzymatic hydrolysis and UF are given in Fig. 5.

4. Conclusions

Enzymatic hydrolysis and UF have been found to be reliable sample pre-treatments for TiO_2 NPs assessment in serum samples. The soft digestion of serum's components by the action of the pancreatin/lipase mixture allows an efficient TiO_2 NPs release so that the extract can be easily analysed by spICP-MS after a previous UF cleaning stage. The mild pH and temperature conditions of enzymatic hydrolysis procedures are very promising for extracting other NPs which could be easily ionized. Therefore, the potential of enzymes as sample pre-treatment tools in nanometrology must be fully realised. Results have demonstrated that the tested UF conditions do not affect TiO_2 NPs size distributions as well as TiO_2 NPs mass concentrations. Although TiO_2 NPs were undetected in the analysed serum samples, our findings show the applicability of spICP-MS for TiO_2 NPs determination/characterization after reliable sample pre-treatments that guarantee the integrity of the TiO_2 NPs. Further research on developing pre-concentration methods is needed for assessing very low TiO_2 NPs number concentration in biofluids. Therefore, the proposed method is a good option for future nanometrological applications in clinical samples.

Table 2
TiO_2 NPs mass concentration and mean size, and analytical recovery for a serum sample subjected to UF and to enzymatic hydrolysis (4.0 h) and UF.

	TiO_2 NPs mass concentration (μg L^{-1})[a]	AR (%)[a,b]	TiO_2 NPs mean size (nm)[a]	TiO_2 NPs most frequent size (nm)[a]
0 h	51.6 ± 5.2	82 ± 8	169 ± 15	146 ± 15
4.0 h	61.1 ± 2.1	97 ± 3	180 ± 7	146 ± 7

(a) n = 3.
(b) TiO_2 NPs mass concentration added 63.5 μg L^{-1}

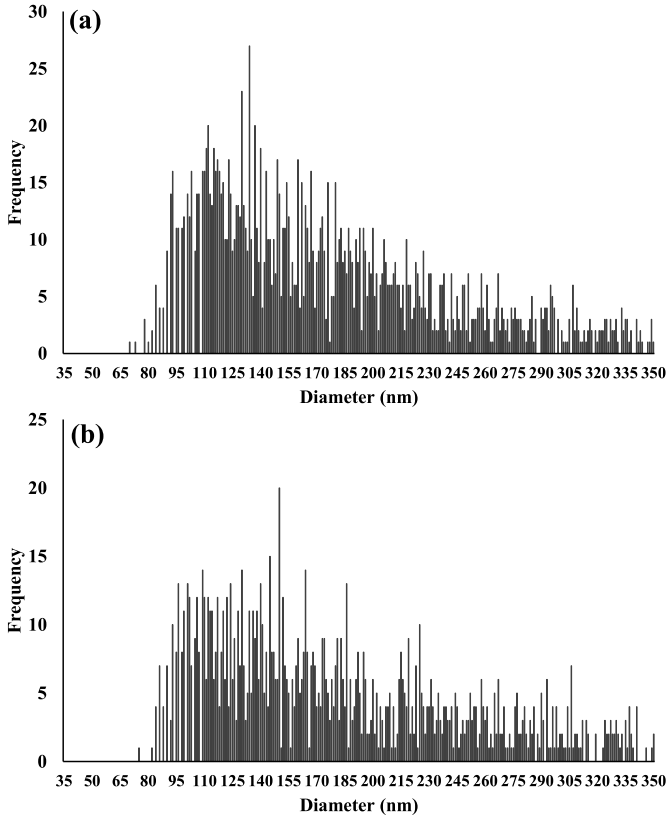

Fig. 4. Histograms for TiO_2 NPs size distribution in a spiked serum sample at 63.5 μg L^{-1} (TiO_2 NPs mass concentration) without enzymatic hydrolysis and with UF (a) and after enzymatic hydrolysis and UF (b).

CRediT authorship contribution statement

Ana Justo-Vega: Writing – original draft, Validation, Software, Formal analysis, Data curation. **Sara Vázquez-Pérez:** Software, Formal analysis, Data curation. **Raquel Domínguez-González:** Writing – original draft, Visualization, Validation, Supervision, Methodology, Investigation. **Pilar Bermejo-Barrera:** Writing – review & editing, Project administration, Funding acquisition, Data curation. **Antonio Moreda-Piñeiro:** Writing – review & editing, Supervision, Project administration, Funding acquisition, Conceptualization.

Funding sources

Grant FOODNANORISK (reference PID2021-125276NB-I00) funded by MICIU/AEI/ 10.13039/501100011033 Spain. and Grupo de Refer encia Competitiva (reference ED431C 2022/029) funded by Consellería de Educacion, ′ Ciencia, Universidades y Formacion ′ Profesional, Xunta de Galicia, Spain. A. J.-V. acknowledges Xunta de Galicia, Spain, for a pre doctoral grant.

Declaration of competing interest

The authors declare that there are no conflicts of interests, and they

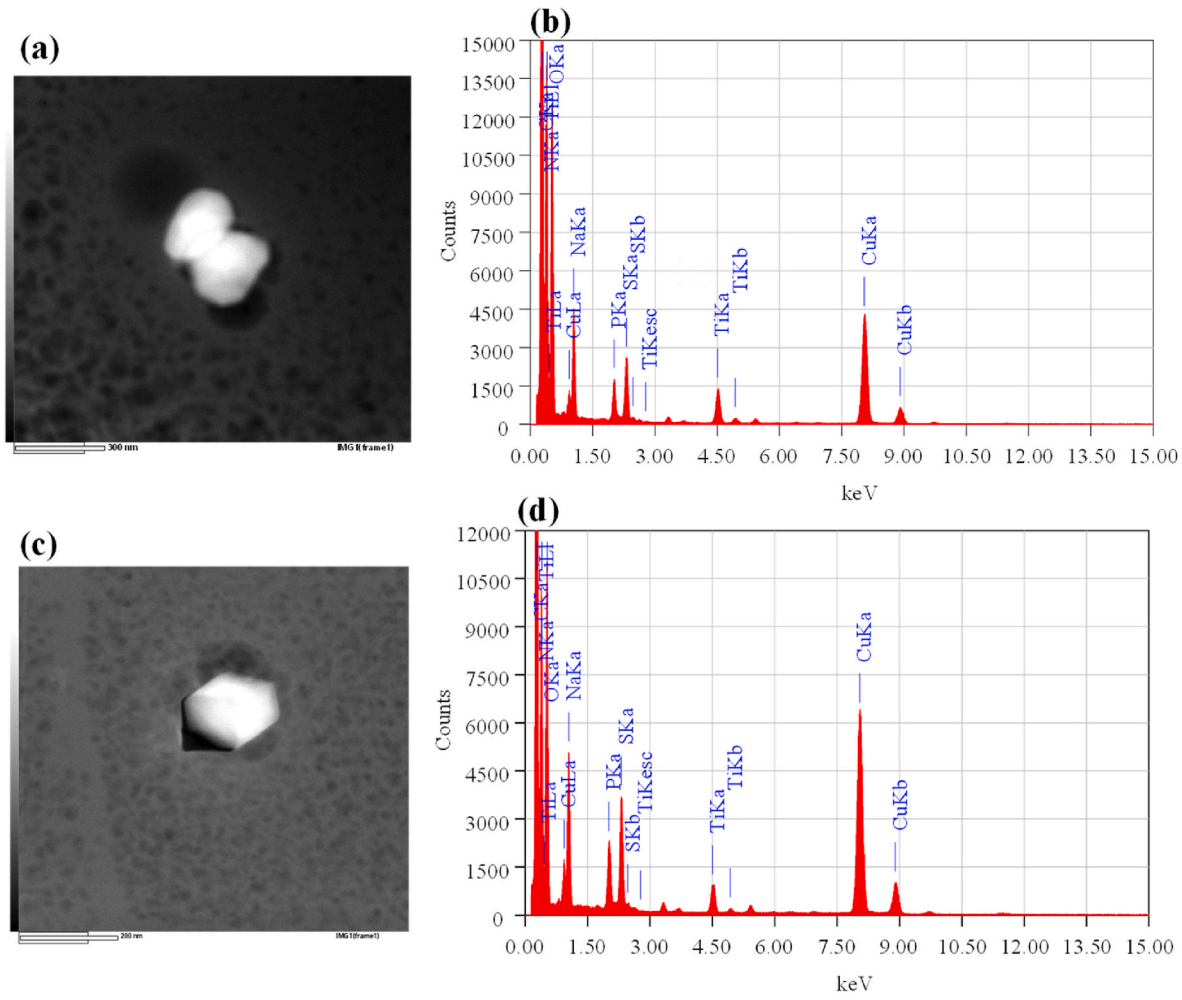

Fig. 5. HRTEM image for spiked serum samples at 63.5 TiO_2 NPs μg L^{-1} without enzymatic hydrolysis and with UF (a) and after enzymatic hydrolysis and UF (c) and EDX spectrum showing Ti characteristic peaks at 4.5 keV (TiK_a) and 5.0 keV (TiK_b) for spiked serum samples at 63.5 TiO_2 NPs μg L^{-1} without enzymatic hydrolysis and with UF (b) and after enzymatic hydrolysis and UF (d).

have no known competing financial interests that could have influenced this work.

Acknowledgments

The authors also wish to María José Pazos-Guldrís from Electronic and Confocal Microscopy and Support for Biological Specialities Unit at the University of Santiago de Compostela for HRTEM-EDX technical support.

Data availability

Data will be made available on request.

References

[1] M.E. Vance, T. Kuiken, E.P. Vejerano, S.P. Mcginnis Jr., M.F. Hochella, D. Rejeski, M.S. Hull, Nanotechnology in the real world: redeveloping the nanomaterial consumer products inventory, J. Nanotechnol. 6 (2015) 1769–1780, https://doi.org/10.3762/bjnano.6.181.

[2] European Food Safety Authority, Safety Assessment of Titanium Dioxide (E171) as a Food Additive, 2021, https://doi.org/10.2903/j.efsa.2021.6585, 01st May. (Accessed 15 March 2024).

[3] European Food Safety Authority, Titanium Dioxide: E171 No Longer Considered Safe when Used as a Food Additive, 2021, 1st May, https://www.efsa.europa.eu/en/news. (Accessed 15 March 2024).

[4] EFSA Scientific Committee, Guidance on risk assessment of nanomaterials to be applied in the food and feed chain: human and animal health, EFSA J. 19 (2021) 6768, https://doi.org/10.2903/j.efsa.2021.6768.

[5] M.V. Taboada-López, G. Vázquez-Expósito, R. González-Domínguez, P. Herbello-Hermelo, P. Bermejo-Barrera y A. Moreda-Piñeiro, Biopersistence rate of metallic nanoparticles in the gastro-intestinal human tract (stage 0 of the EFSA guidance for nanomaterials risk assessment), Food Chem. 360 (2021) 130002, https://doi.org/10.1016/j.foodchem.2021.130002.

[6] M. Ferrante, A. Grasso, G. Giuberti, M. Dall'Asta, E. Puglisi, G. Arena, A. Nicosia, M. Fiore, C. Copat, Behaviour and fate of Ag-NPs, TiO_2-NPs and ZnO-NPs in the human gastrointestinal tract: biopersistence rate evaluation, Food Chem. Toxicol. 176 (2023) 113779, https://doi.org/10.1016/j.fct.2023.113779.

[7] E. Espada-Bernabé, G. Moreno-Martín, B. Gómez-Gómez, Y. Madrid, Assessing the behaviour of particulate/nanoparticulate form of E171 (TiO_2) food additive in colored chocolate candies before and after in vitro oral ingestion by spICP-MS, TEM and cellular in vitro models, Food Chem. 432 (2024) 13720, https://doi.org/10.1016/j.foodchem.2023.137201.

[8] M. Hemmendinger, G. Squillacioti, T. Charreau, G. Garzaro, F. Ghelli, R. Bono, J.-J. Sauvain, G. Suarez, N.B. Hopf, P. Wild, A. Progiou, C. Fito, E. Bergamaschi, I. G. Canu, Occupational exposure to nanomaterials and biomarkers in exhaled air and urine: insights from the NanoExplore international cohort, Environ. Int. 179 (2023) 108157, https://doi.org/10.1016/j.envint.2023.108157.

[9] B. Bocca, B. Battistini, V. Leso, L. Fontana, S. Caimi, M. Fedele, I. Iavicoli, Occupational exposure to metal engineered nanoparticles: a Human biomonitoring pilot study involving Italian nanomaterial workers, Toxics 11 (2023) 120, https://doi.org/10.3390/toxics11020120.

[10] N. Hadrup, A.K. Sharma, Katrin Loeschner, Toxicity of silver ions, metallic silver, and silver nanoparticle materials after in vivo dermal and mucosal surface exposure: a review, Regul. Toxicol. Pharmacol. 98 (2018) 257–267, https://doi.org/10.1016/j.yrtph.2018.08.007.

[11] C. Contado, Nanomaterials in consumer products: a challenging analytical problem, Front. Chem. 3 (2015) 48, https://doi.org/10.3389/fchem.2015.00048.

[12] S. Fernández-Trujillo, M. Jiménez-Moreno, N. Rodríguez-Fariñas, R.C. Rodríguez Martín-Doimeadios, Critical evaluation of the potential of ICP-MS-based systems in toxicological studies of metallic nanoparticles, Anal. Bioanal. Chem. 416 (2024) 2657–2676, https://doi.org/10.1007/s00216-024-05181-4.
[13] X. Tian, H. Jiang, L. Hu, M. Wang, W. Cui, J. Shi, G. Liu, Y. Yin, Y. Cai, G. Jiang, Simultaneous multi-element and multi-isotope detection in single-particle ICP-MS analysis: principles and applications, Trends Anal. Chem. 157 (2022) 116746, https://doi.org/10.1016/j.trac.2022.116746.
[14] D. Mozhayeva, C. Engelhard, A critical review of single particle inductively coupled plasma mass spectrometry – a step towards an ideal method for nanomaterial characterization, J. Anal. At. Spectrom. 35 (2020) 1740–1783, https://doi.org/10.1039/c9ja00206e.
[15] K. Loeschner, M.E. Johnson, A.R. Montoro Bustos, Application of single particle ICP-MS for the determination of inorganic nanoparticles in food additives and food: a short review, Nanomaterials 13 (2023) 2547, https://doi.org/10.3390/nano13182547.
[16] M. Witzler, F. Küllmer, K. Günther, Validating a Single-particle ICP-MS method to measure nanoparticles in human whole blood for nanotoxicology, Anal. Lett. 51 (2018) 587–599, https://doi.org/10.1080/00032719.2017.1327538.
[17] B. Bocca, B. Battistini, F. Petrucci, Silver and gold nanoparticles characterization by SP-ICP-MS and AF4-FFF-MALS-UV-ICP-MS in human samples used for biomonitoring, Talanta 220 (2020) 121404, https://doi.org/10.1016/j.talanta.2020.121404.
[18] M. Cabré, G. Fernández, E. González, J. Abellà, A. Verdaguer, Single particle ICP-MS: a tool for the characterization of gold nanoparticles in nanotheranostics applications, J. Anal. At. Spectrom. 39 (2024) 2508, https://doi.org/10.1039/d4ja00141a.
[19] I. Abad-Alvaro, D. Leite, D. Bartczak, S. Cuello-Nunez, B. Gomez-Gomez, Y. Madrid, M. Aramendia, M. Resano, H. Goenaga-Infante, An insight into the determination of size and number concentration of silver nanoparticles in blood using single particle ICP-MS (spICP-MS): feasibility of application to samples relevant to in vivo toxicology studies, J. Anal. At. Spectrom. 36 (2021) 1180, https://doi.org/10.1039/d1ja00068c.
[20] M. Roman, C. Rigo, H. Castillo-Michel, I. Munivrana, V. Vindigni, I. Mičetić, F. Benetti, L. Manodori, W.R.L. Cairns, Hydrodynamic chromatography coupled to single-particle ICP-MS for the simultaneous characterization of AgNPs and determination of dissolved Ag in plasma and blood of burn patients, Anal. Bioanal. Chem. 408 (2016) 5109–5124, https://doi.org/10.1007/s00216-015-9014-6.
[21] K. Badalova, P. Herbello-Hermelo, P. Bermejo-Barrera, A. Moreda-Piñeiro, Possibilities of single particle—ICP-MS for determining/characterizing titanium dioxide and silver nanoparticles in human urine, J. Trace Elem. Med. Biol. 54 (2019) 55–61, https://doi.org/10.1016/j.jtemb.2019.04.003.
[22] S. Fernández-Trujillo, M. Jiménez-Moreno, Á. Ríos, R.C. Rodríguez Martín-Doimeadios, A simple analytical methodology for platinum nanoparticles control in complex clinical matrices via SP-ICP-MS, Talanta 231 (2021) 122370, https://doi.org/10.1016/j.talanta.2021.122370.
[23] S. Salou, D. Larivière, C.-M. Cirtiu, N. Fleury, Quantification of titanium dioxide nanoparticles in human urine by single-particle ICP-MS, Anal. Bioanal. Chem. 413 (2021) 171–181, https://doi.org/10.1007/s00216-020-02989-8.
[24] J. Kruszewska, J. Sikorski, J. Samsonowicz-Górski, M. Matczuk, A CE-ICP-MS/MS method for the determination of superparamagnetic iron oxide nanoparticles under simulated physiological conditions, Anal. Bioanal. Chem. 412 (2020) 8145–8153, https://doi.org/10.1007/s00216-020-02948-3.
[25] K. Mehrabi, M. Dengler, I. Nilsson, M. Baumgartner, C.A. Mora, D. Günther, A. Gundlach-Graham, Detection of magnetic iron nanoparticles by single-particle ICP-TOFMS: case study for a magnetic filtration medical device, Anal. Bioanal. Chem. 414 (2022) 6743–6751, https://doi.org/10.1007/s00216-022-04234-w.
[26] M.V. Taboada-López, S. Iglesias-López, P. Herbello-Hermelo, P. Bermejo-Barrera, A. Moreda-Piñeiro, Ultrasound assisted enzymatic hydrolysis for isolating titanium dioxide nanoparticles from bivalve mollusk before sp-ICP-MS, Anal. Chim. Acta 1018 (2018) 16–25, https://doi.org/10.1016/j.aca.2018.02.075.
[27] M.V. Taboada-López, P. Herbello-Hermelo, R. Domínguez-González, P. Bermejo-Barrera, A. Moreda-Piñeiro, Enzymatic hydrolysis as a sample pre-treatment for titanium dioxide nanoparticles assessment in surimi (crab sticks) by single particle ICP-MS, Talanta 195 (2019) 23–32, https://doi.org/10.1016/j.talanta.2018.11.023.
[28] M.V. Taboada-López, N. Alonso-Seijo, P. Herbello-Hermelo, P. Bermejo-Barrera, A. Moreda-Piñeiro, Determination and characterization of silver nanoparticles in bivalve molluscs by ultrasound assisted enzymatic hydrolysis and sp-ICP-MS, Microchem. J. 148 (2019) 652–660, https://doi.org/10.1016/j.microc.2019.05.023.
[29] C. Suárez-Oubiña, P. Herbello-Hermelo, N. Mallo, M. Vázquez, S. Cabaleiro, R. Domínguez-González, A. Moreda-Piñeiro, P. Bermejo-Barrera, Bioaccumulation and human risk assessment of inorganic nanoparticles in aquaculture species, Environ. Sci. Nano 11 (2024) 2937–2947, https://doi.org/10.1039/D4EN00167B.
[30] Y. Dan, W. Zhang, R. Xue, X. Ma, C. Stephan, H. Shi, Characterization of gold nanoparticle uptake by tomato plants using enzymatic extraction followed by single-particle inductively coupled plasma−mass spectrometry analysis, Environ. Sci. Technol. 49 (2015) 3007–3014, https://doi.org/10.1021/es506179e.
[31] J.J. López-Mayán, B. Álvarez-Fernández, E. Peña-Vázquez, M.C. Barciela-Alonso, A. Moreda-Piñeiro, P. Bermejo-Barrera, Ultrasonication followed by enzymatic hydrolysis as a sample pre-treatment for the determination of Ag nanoparticles in edible seaweed by SP-ICP-MS, Talanta 247 (2022) 123556, https://doi.org/10.1016/j.talanta.2022.123556.
[32] J.J. López-Mayán, B. Álvarez-Fernández, E. Peña-Vázquez, M.C. Barciela-Alonso, A. Moreda-Piñeiro, J. Maguire, M. Mackey, M. Quarato, I. Pinheiro, B. Espiña, L. Rodríguez-Lorenzo, P. Bermejo-Barrera, Bioaccumulation of titanium dioxide nanoparticles in green (*Ulva sp.*) and red (*Palmaria palmata*) seaweed, Microchim. Acta 190 (2023) 287, https://doi.org/10.1007/s00604-023-05849-1.
[33] C. Suárez-Oubiña, P. Herbello-Hermelo, P. Bermejo-Barrera, A. Moreda-Piñeiro, Single-particle inductively coupled plasma mass spectrometry using ammonia reaction gas as a reliable and free-interference determination of metallic nanoparticles, Talanta 242 (2022) 123286, https://doi.org/10.1016/j.talanta.2022.123286.
[34] H.E. Pace, N.J. Rogers, C. Jarolimek, V.A. Coleman, C.P. Higgins, J.F. Ranville, Determining transport efficiency for the purpose of counting and sizing nanoparticles via single particle inductively coupled plasma mass spectrometry, Anal. Chem. 83 (24) (2011) 9361–9369, https://doi.org/10.1021/ac201952t.
[35] A. Poletaev, Composition of the blood and reflection of the health state of human body, Biomed. Pharmacol. J. 11 (2018) 1797–1800, https://doi.org/10.13005/bpj/1551.
[36] V.R. Sharma, Aggregation and toxicity of titanium dioxide nanoparticles in aquatic environment—a Review, J. Environ. Sci. Health, Part A 44 (2009) 1485–1495, https://doi.org/10.1080/10934520903263231.
[37] G.E. Schaumann, A. Philippe, M. Bundschuh, G. Metreveli, S. Klitzke, D. Rakcheev, A. Grün, S.K. Kumahor, M. Kühn, T. Baumanng, F. Lang, W. Manz, R. Schulz, H.-J. Vogel, Understanding the fate and biological effects of Ag- and TiO_2-nanoparticles in the environment: the quest for advanced analytics and interdisciplinary concepts, Sci. Total Environ. 535 (2015) 3–19, https://doi.org/10.1016/j.scitotenv.2014.10.035.
[38] F. Xu, Review of analytical studies on TiO_2 nanoparticles and particle aggregation, coagulation, flocculation, sedimentation, stabilization, Chemosphere 212 (2018) 662–677, https://doi.org/10.1016/j.chemosphere.2018.08.108.
[39] J.J. López-Mayán, S. del-Ángel-Monroy, E. Peña-Vázquez, M.C. Barciela-Alonso, P. Bermejo-Barrera, A. Moreda-Piñeiro, Titanium dioxide nanoparticles assessment in seaweeds by single particle inductively coupled plasma – mass spectrometry, Talanta 236 (2022) 122856, https://doi.org/10.1016/j.talanta.2021.122856.
[40] F. Laborda, A.C. Gimenez-Ingalaturre, E. Bolea, J.R. Castillo, About detectability and limits of detection in single particle inductively coupled plasma mass spectrometry, Spectrochim. Acta, Part B 169 (2020) 105883, https://doi.org/10.1016/j.sab.2020.105883.
[41] F. Laborda, J. Jiménez-Lamana, E. Bolea, J.R. Castillo, Critical considerations for the determination of nanoparticle number concentrations, size and number size distributions by single particle ICP-MS, J. Anal. At. Spectrom. 28 (2013) 1220–1232, https://doi.org/10.1039/C3JA50100K.